Parity oscillations and photon correlation functions in the Z_{2}-U(1) Dicke model at a finite number of atoms or qubits

Yu Yi-Xiang, Jinwu Ye, and CunLin Zhang

Phys. Rev. A **94**, 023830 — Published 17 August 2016

DOI: 10.1103/PhysRevA.94.023830

Parity oscillations and photon correlation functions in the $Z_2/U(1)$ Dicke model at a finite number of atoms or qubits

Yu Yi-Xiang[1,2,3], Jinwu Ye [1,2,4] and CunLin Zhang [1]

[1] *Department of Physics, Capital Normal University, Key Laboratory of Terahertz Optoelectronics, Ministry of Education, and Beijing Advanced innovation Center for Imaging Technology, Beijing, 100048, China*

[2] *Department of Physics and Astronomy, Mississippi State University, P. O. Box 5167, Mississippi State, MS, 39762*

[3] *School of Instrument Science and Opto-electronics Engineering, Institute of Optics and Electronics, BeiHang University, Beijing 100191, China*

[4] *Kavli Institute of Theoretical Physics, University of California, Santa Barbara, Santa Barbara, CA 93106*

The four standard quantum optics models such as Rabi, Dicke, Jaynes-Cummings (JC) and Tavis-Cummings (TC) model were proposed by the old generation of great physicists many decades ago. Despite their relative simple forms and many previous theoretical works, their physics at a finite N, especially inside the superradiant regime, remain unknown. In this work, by using the strong coupling expansion and exact diagonization (ED), we study the $Z_2/U(1)$ Dicke model with independent rotating wave (RW) coupling g and counter-rotating wave (CRW) coupling g' at a finite N. This model includes the four standard quantum optics models as its various special limits. We show that in the super-radiant phase, the system's energy levels are grouped into doublets with even and odd parity. Any anisotropy $\beta = g'/g \neq 1$ leads to the oscillation of parities in both the ground and excited doublets as the atom-photon coupling strength increases. The oscillations will be pushed to the infinite coupling strength in the isotropic Z_2 limit $\beta = 1$. We find nearly perfect agreements between the strong coupling expansion and the ED in the super-radiant regime when β is not too small. We also compute the photon correlation functions, squeezing spectrum, number correlation functions which can be measured by various standard optical techniques.

I. INTRODUCTION

There are several well known quantum optics models to study atom-photon interactions[1, 2]. In the Rabi model[3], a single photon mode interacts with a two level atom with equal rotating wave (RW) and counter rotating wave (CRW) strength. When the coupling strength is well below the transition frequency, the CRW term is effectively much smaller than that of RW, so it was dropped in the Jaynes-Cummings (JC) model [4]. Then the Rabi and JC model were extended respectively to the Dicke model [5] and the Tavis-Cummings (TC) model [6] with an assembly of N two-level atoms. Despite their relative simple forms and many previous theoretical works [10–15], their solutions at a finite N, especially inside the superradiant regime, remain unknown. Here, we address this outstanding problem. It is convenient to classify the four well known quantum optics models from a simple symmetry point of view: the TC and Dicke model as the $U(1)$ and Z_2 Dicke model [7–9] respectively, while JC and Rabi model are just as the $N = 1$ version of the two.

Due to recent tremendous advances in technologies, ultra-strong couplings in cavity QED systems were achieved in at least two experimental systems (1) a BEC atoms inside an ultrahigh-finesse optical cavity [16–20] and (2) superconducting qubits inside a microwave circuit cavity [21–23, 25] or quantum dots inside a semiconductor microcavity [24]. In general, in such a ultra-strong coupling regime, the system is described well by Eq.1 dubbed as the $U(1)/Z_2$ Dicke model [8, 26, 27] which includes the four standard quantum optics models as its various special limits. Despite many previous theoretical works on its various special limits [10–15], their solutions at a finite N, especially inside the superradiant regime, remain unknown. Here, we address this outstanding problem. Specifically, we study the $U(1)/Z_2$ Dicke model Eq.1 at any finite N and any ratio $0 \leq g'/g = \beta \leq 1$ between the Rotating wave (RW) term g and the counter rotating wave (CRW) term g' by the strong coupling expansion [28] and exact diagonization (ED) [8, 12, 29]. We show that in the super-radiant phase, the system's energy levels are grouped into doublets with the even and odd parities, respectively. Any anisotropy $\beta \neq 1$ leads to the oscillation of parities in the ground and excited doublet states in superradiant phase as the g increases. In the Z_2 limit $\beta = 1$, all the oscillations are pushed to $g = \infty$. We find nearly perfect agreements between the strong coupling expansion and the ED in the super-radiant regime when β is not too small. We compute the photon correlation functions, squeezing spectrum and number correlation functions which can be detected by fluorescence spectrum, phase sensitive homodyne detection and Hanbury-Brown-Twiss (HBT) type of experiments respectively [1, 2, 30]. Experimental realizations are discussed. New perspectives are outlined.

II. STRONG COUPLING EXPANSION

In the strong coupling limit, it is more convenient to start from the Z_2 limit with $\beta = 1$, then treat $1 - \beta$ as a small parameter, one can rewrite the $U(1)/Z_2$ Dicke model [8] in its dual $Z_2/U(1)$ presentation:

$$H_{Z_2/U(1)} = \omega_a a^\dagger a + \omega_b J_z + \frac{g(1+\beta)}{\sqrt{N}}(a^\dagger + a)J_x - \frac{g(1-\beta)}{\sqrt{N}}(a^\dagger - a)iJ_y \quad (1)$$

where ω_a, ω_b are the cavity photon frequency and the energy difference of the two atomic levels respectively, the g and $g' = \beta g, 0 \leq \beta \leq 1$ are the atom-photon rotating wave (RW) and the counter-rotating wave (CRW) coupling respectively. If $\beta = 0$, Eq.1 reduces to the $U(1)$ Dicke model [7–9] with the $U(1)$ symmetry $a \to ae^{i\theta}, \sigma^- \to \sigma^- e^{i\theta}$ leading to the conserved quantity $P = a^\dagger a + J_z$. The CRW g' term breaks the $U(1)$ to the Z_2 symmetry $a \to -a, \sigma^- \to -\sigma^-$ with the conserved parity operator $\Pi = e^{i\pi(a^\dagger a + J_z)}$. If $\beta = 1$, it becomes the Z_2 Dicke model [12, 13, 31].

After performing a rotation around the J_y axis by $\pi/2$, one can write $H = H_0 + V$ where $H_0 = \omega_a[a^\dagger a + G(a^\dagger + a)J_z], G = \frac{g(1+\beta)}{\omega_a\sqrt{N}}$ and the perturbation $V = -\frac{\omega_b}{2}[J_+(1 + \lambda(a^\dagger - a)) + J_-(1 - \lambda(a^\dagger - a))]$ where $\lambda = \frac{g(1-\beta)}{\omega_b\sqrt{N}}$ is a dimensionless parameter of order 1 when $1-\beta$ is small in the large g limit. In principle, the strong coupling expansion is performed in the large g limit $G \gg 1$, but with a small $1-\beta$ such that λ is of order 1. In practice, as compared to ED, the method works well also when g is not too close to $g_c = \frac{\sqrt{\omega_a\omega_b}}{1+\beta}$ and β is not too close to the $U(1)$ limit $\beta = 0$.

Define $A = a + GJ_z$, then $H_0 = \omega_a[A^\dagger A - (GJ_z)^2]$ [29]. Because $[A, J_z] = 0$, we denote the simultaneous eigenstates of A and J_z as $|l\rangle_m|jm\rangle, m = -j, \cdots, j, l = 0, 1, \cdots$. The eigenstates satisfy $J_z|jm\rangle = m\hbar|jm\rangle, A_m^\dagger A_m|l\rangle_m = l|l\rangle_m$ where $A_m = a + Gm$, $|l\rangle_m = D^\dagger(g_m)|l\rangle = D(-g_m)|l\rangle$ where $D(\alpha) = e^{\alpha a - \alpha^* a^\dagger}, g_m = mG$ and $|l\rangle$ is just the l-photon Fock state. Particularly, the ground state $|0\rangle_m = D(-g_m)|0\rangle$ is a photon coherent state. The zeroth order eigen-energies are $H_0|l\rangle_m|jm\rangle = E^0_{l,m}|jm\rangle, E^0_{l,m} = \omega_a(l - g_m^2)$. Using the parity operator $\Pi = e^{i\pi(a^\dagger a - J_x)}$, one can show that $\Pi|l\rangle_m|jm\rangle = (-1)^l|l\rangle_{-m}|j,-m\rangle$. Because the parity is a conserved quantity at any finite N, one can group all the eigenstates into even or odd under the parity operator $\Pi = e^{i\pi(a^\dagger a - J_x)}$:

$$|e\rangle = \frac{1}{\sqrt{2}}[|l\rangle_m|j,m\rangle + (-1)^l|l\rangle_{-m}|j,-m\rangle]$$
$$|o\rangle = \frac{1}{\sqrt{2}}[|l\rangle_m|j,m\rangle - (-1)^l|l\rangle_{-m}|j,-m\rangle] \quad (2)$$

The ground state is a doublet at $|l = 0\rangle_{\pm j}|j, \pm j\rangle$. In the large g limit, the excited states can be grouped into two sectors: (1) The atomic sector with the eigenstates $|l > 0\rangle_{\pm j}|j, \pm j\rangle$ with the energies $l\omega_a$. The first excited state $l = 1$ with the energy ω_a is the remanent of the pseudo-Goldstone mode in the $U(1)$ regime [8]. (2) The optical sector with the eigenstates $|l\rangle_m|j,m\rangle, |m| < j$. The first excited state has the energy $\omega_o = E^0_{l,m=j-1} - E^0_{l,m=j} = \omega_a G^2(2j-1) = \frac{g^2(1+\beta)^2}{\omega_a}(\frac{2j-1}{2j})$ and is the remanent of the Higgs mode in the $U(1)$ regime [8]. So in the strong coupling limit, there is wide separation between the atomic sector and the optical sector. This makes the strong coupling expansion very effective to explore the physical phenomena in the superradiant regime.

III. GROUND STATE ($l = 0$) SPLITTING

The two degenerate ground state are $|1\rangle = |l = 0\rangle_{-j}|j, -j\rangle, |2\rangle = |l = 0\rangle_j|j, j\rangle$ with the zeroth order energy $E_0 = -\omega_a(Gj)^2$. Then we can determine the matrix elements in the 2×2 matrix which is the effective Hamiltonian projected onto the 2 dimensional subspace. By a second order perturbation, one finds a non-zero diagonal matrix element:

$$V_{11} = V_{22} = V_0(\lambda) = -\frac{\omega_b^2}{\omega_a}\frac{2j}{2j-1}\frac{1+\lambda^2}{G^2} < 0 \quad (3)$$

However, one needs to perform a $N = 2j$ order perturbation (See appendix A) to find the first non-zero contribution to the off-diagonal matrix element $V_{12} = V_{21} = \Delta_0(\lambda)$:

$$\Delta_0(\lambda) = -\frac{N^2\omega_b}{2}(\frac{\omega_b}{2\omega_a G^2})^{N-1}e^{-(NG)^2/2} \times \sum_{l=0}^{N}\frac{\lambda^l}{(N-l)!}\sum_{n=0}^{[l/2]}\frac{(-1/2)^n(-NG)^{l-2n}}{n!(l-2n)!} \quad (4)$$

where $[l/2]$ is the closest integer to $l/2$ and $\frac{\lambda}{G} = \frac{1-\beta}{1+\beta}\frac{\omega_a}{\omega_b}$.

Setting $\lambda = 0$ in Eq.4 leads to the splitting in the Z_2 Dicke model at $\beta = 1$ (Fig.2d):

$$\Delta_0 = -\frac{\omega_b}{(N-1)!}(\frac{\omega_b}{2\omega_a})^{N-1}\frac{2g^2}{\omega_a^2}e^{-N\frac{2g^2}{\omega_a^2}} < 0 \quad (5)$$

which is always a negative quantity, so leads to the even and odd parity as the ground state and the excited state in the $l = 0, m = j$ doublet in Eq.2 having the energies $E_{o/e} = E_0 + V_0 \pm |\Delta_0|$ (Fig.1).

Now we study the dramatic effects of the anisotropy $\lambda > 0$ encoded in Eq.4. If removing the exponential factor $e^{-(G')^2/2}$ where $G' = NG$, Eq.4 is a $2N$-th polynomial of g. We find that it always has N positive zeros in g beyond the g_c (namely, fall into the super-radiant regime). Higher than the $N-$th order perturbations will lead to other zeros at larger g shown in Fig.3b. Any changing of sign in $\Delta_0(\lambda)$ leads to the exchange of the parity in the ground state $l = 0, m = j$ in Eq.2 (namely, Eq.B1) with the energies $E_{o/e} = E_0 + V_0(\lambda) \pm |\Delta_0(\lambda)|$ in Fig.1. So any $\lambda > 0$ will lead to infinite number of level crossings with alternative parities in the ground state, which is indeed observed in the ED results Fig.2 for the energy levels at $N = 2$ and $\beta = 0.1, 0.5, 0.9$. It is the anisotropy

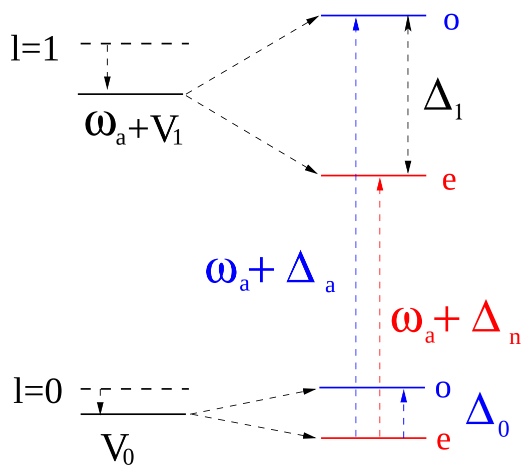

FIG. 1. (Color Online) The energy shifts $V_0 < 0, V_1 < 0$ and splittings Δ_0, Δ_1 of the ground state $l = 0$ and the first excited state $l = 1$. Shown here is $\Delta_0 < 0, \Delta_1 > 0$ case where the even parity state is the ground state at $l = 0, 1$. The blue and red dashed transition lines can be mapped out by photon and photon number correlation functions Eq.10 and 11 respectively.

which leads to the parity oscillations in the superradiant regime. However, at $\beta = 1$, the infinite level crossings are pushed to infinity, so no parity oscillations in Fig.2d anymore [31].

IV. DOUBLET SPLITTING AT EXCITED STATES $l > 0$

Now, we look at the energy splitting at $l > 0$. The diagonal matric element at $l = 0$ in Eq.3 can be easily generalized to $l > 0$ case:

$$V_{11} = V_{22} = V_l(\lambda) = -\frac{\omega_b^2}{\omega_a}\frac{2j}{2j-1}\frac{1+\lambda^2(2l+1)}{G^2} < 0 \quad (6)$$

By performing a $N = 2j$ order perturbation, we also find a general (but a little bit complicated) expression for the off-diagonal matrix element $V_{12} = V_{21} = \Delta_l(\lambda)$.

However, in the $G \gg 1$ limit, it can be simplified to:

$$\Delta_l(\lambda) \sim \frac{(-1)^l}{l!}(G'^2)^l \Delta_0(\lambda) \quad (7)$$

where $\Delta_0(\lambda)$ is given in Eq.4. It is enhanced due to the large prefactor G'^{2l}. Note that it is this oscillating sign $(-1)^l$ which leads to the even/odd parity state with an extra $(-1)^l$ in Eq.2 with $m = j$ (namely Eq.B2). The l-th levels have the energies $E_{o/e} = E_l^0 + V_l(\lambda) \pm |\Delta_l(\lambda)|, E_l^0 = \omega_a[l - (Gj)^2]$ with $l = 1$ shown in Fig.1. The diagonal part of the excited energy is:

$$\begin{aligned}(E_l^0 + V_l(\lambda)) - (E_0^0 + V_0(\lambda)) &= l\omega_a - (|V_l| - |V_0|) \\ &= l\omega_a - \frac{\omega_b^2}{\omega_a}\frac{2j}{2j-1}\frac{1+2\lambda^2}{G^2} < l\omega_a \quad (8)\end{aligned}$$

which approaches $l\omega_a$ from below in the $G \gg 1$ limit. This is indeed confirmed by the ED in Fig.2.

Eq.7 shows that at the N-th order perturbation, the number of zeros remains to be N and the positions of the zeros are independent of l in the $G \gg 1$ limit. This observation is indeed confirmed in the following ED results in Fig.3.

V. EXACT DIAGONIZATION RESULTS

Due to the λ term in Eq.1, it is not convenient to perform the ED in the coherent basis anymore used in [29], so we did the ED in the original (Fock) basis [12]. In the Fock space, the complete basis is $|n\rangle|j,m\rangle, n = 0, 1, 2, ...\infty, j = N/2, m = -j, ..., j$ where the n is the number of photons and the $|j,m\rangle$ is the Dicke states. In performing the ED, following [12], one has to use a truncated basis $n = 0, 1, ...n_c$ in the photon sector where the $n_c \sim 100$ is the maximum photon number in the artificially truncated Hilbert space. As long as the low energy levels in Fig.3 and Fig.2 are well below $n_c\omega_a$, then the energy levels should be very close to the exact results without the truncation (namely, sending $n_c \to \infty$). However, the ED may not be precise anymore when g gets too close to the upper cutoff introduced in the ED calculations as shown in Fig.3c.

VI. COMPARISON BETWEEN THE STRONG COUPLING EXPANSION AND THE EXACT DIAGONZIATION (ED)

In Fig.3 (a)-(c), we compare Eq.4 and 7 with the ED results on the energy level splitting between the doublets with even and odd parity for $N = 2$ at $\beta = 0.1, 0.5, 0.9, l = 0, 1, 2$. We find the first N zeros (or parity oscillations) from the strong coupling expansion match those from the ED nearly perfectly well at $\beta = 0.5, 0.9$ in the super-radiant regime. Of course, the ED may not be precise anymore when g gets too close to the upper cutoff introduced in the ED calculation as shown in Fig.3d. In fact, the first $N = 2$ zeros of Eq.4 can be found exactly as the two positive roots:

$$G_{\mp} = (\sqrt{1 + 8\frac{1+\beta}{1-\beta}} \mp 1)/4 \quad (9)$$

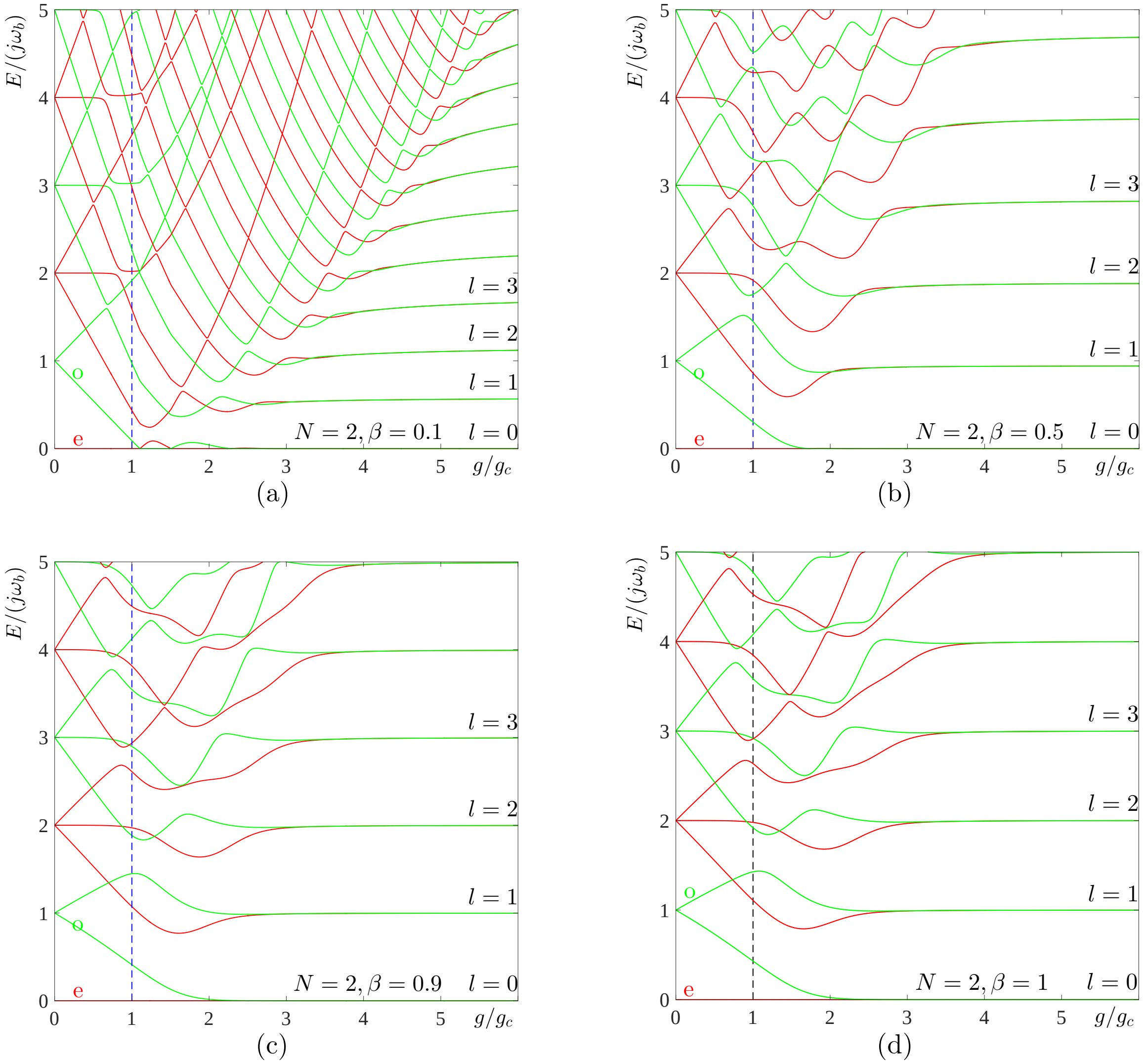

FIG. 2. (Color Online) ED results for the energy levels at $N=2$ and $\beta=0.1, 0.5, 0.9$ and also the Z_2 limit $\beta=1$ in (a)-(d) respectively. For simplicity, we only show $\omega_a=\omega_b$ case. The parity even (e) in red color and odd (o) in green color are indicated. We only label the atomic modes $l=0,1,2,3....$ There are none, one and two level crossing(s) in the normal regime at $l=0,1,2$ respectively. When expanding the doublets at $l=0,1,....$, as g/g_c increases, there are infinite energy level crossings leading to the oscillations of parities at the ground states at $l=0,1,....$ manifolds shown in Fig.3. As $\beta\to 1^-$, all the zeros are pushed to infinity in (d). There are no level crossings anymore between the even and odd parity pairs. Only the atomic energies at $l=0,1,2....$ are labeled. As $g/g_c\to\infty$ limit, they approach to $l\omega_a$ from below. This behavior has been discovered by the strong coupling expansion in the main text. Note that the energy levels here are not directly experimental detectable. But the photon correlations functions listed in Eq.10 and 11 are.

which falls in the superradiant regime. The spacing between the two roots $\Delta(\frac{g}{g_c})=\frac{1}{\sqrt{2}}$ is independent of β as shown in Fig.3c,d. As $\beta\to 1^-$, both roots $\sim(1-\beta)^{-1/2}$ are pushed into the infinity.

Eq.7 is also confirmed by the ED shown in Fig.3d for $N=2, \beta=0.9, l=0,1,2$ where the positions of the first $N=2$ zeros only depend on l very weakly. So between the two zeros, at $l=0,1,2,\cdots$, the energy levels are in the pattern $(e,o),(e,o),\cdots$ when $\Delta_0(\lambda)<0$ shown in Fig.1 (or $(o,e),(o,e),\cdots$ when $\Delta_0(\lambda)>0$).

VII. PHOTON, SQUEEZING AND NUMBER CORRELATION FUNCTIONS

Note that the energy level structures in Fig.3a-c are not directly experimentally measurable. So it is very important to evaluate various photon correlation functions

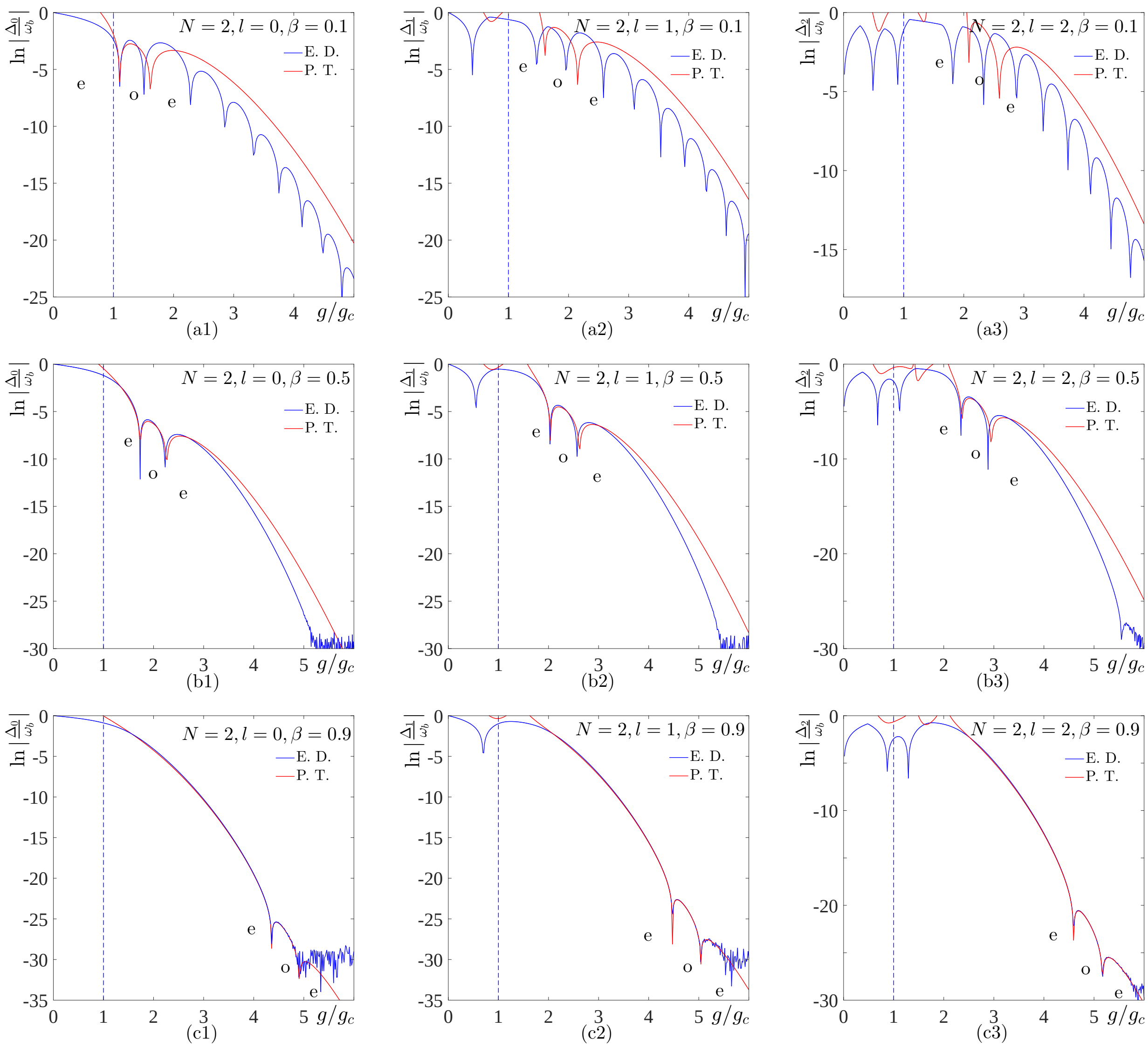

FIG. 3. (Color Online) Shown in (a)-(c) are the even/odd splitting Δ_l for $N=2$ at $\beta=0.1, 0.5, 0.9$ and $l=0,1,2$ in the Log scale $\ln|\frac{\Delta_l}{\omega_b}|$ versus g/g_c. The labels e and o are the parity of the ground states. Being $\Delta_0>0$, the ground state between the first two zeros in (a)-(c) has the odd parity. The red (blue) line is from the strong coupling expansion and the ED. The numerical sharp dips mean the zero splittings. It always starts with the even parity with oscillating parities at $l=0,1,2$. There are also none, one and two level crossing(s) in the normal regime at $l=0,1,2$. The ED gives infinite number of zeros after the first $N=2$ zeros which can only be achieved from higher order perturbations in the strong coupling expansion. In (a) at $\beta=0.1$, the strong coupling results match well with those from the ED at $l=0$, but not too well at $l=1,2$ in the first $N=2$ zeros. Even so, they match well the envelop of the splitting at $l=0,1,2$ (namely, the maximum splitting). In both (b) and (c), the strong coupling results match very well with those from ED in the first $N=2$ zeros. The other zeros are far apart from the first $N=2$ zeros and out of the scope in the figure. In (a) or (b), if one follow the ground state with the odd parity, there are some or slight shifts of zeros to the right at $l=0,1,2$. In (c), the shifts are very small as dictated by Eq.7 in the limit $G=\frac{g}{g_c}\frac{1}{\sqrt{N}}\gg 1$. At too strong couplings, the ED may become (noise) un-reliable due to the cutoff introduced in the ED.

graphically shown in Fig.1, which can be directly measured through leaking cavity photons by various standard quantum optics detection methods. In order to calculate the photon correlation functions in the strong coupling limit, one not only needs to find the energy levels as done in the previous sections and in Fig.1, but also the wavefunctions listed in the appendix B. Using the Lehmann representations, we find there is no first order correction to the normal photon correlation function, but there is one $\sim 1/G^2$ to the anomalous photon correlation function:

$$\begin{aligned}\langle a(t)a^\dagger(0)\rangle &= Ae^{-i|\Delta_0|t}+e^{-i(\omega_a+\Delta_a)t}\\ \langle a(t)a(0)\rangle &= Ae^{-i|\Delta_0|t}-Be^{-i(\omega_a+\Delta_a)t}\end{aligned} \tag{10}$$

where $A=(Gj)^2=N\frac{g^2(1+\beta)^2}{4\omega_a^2}\sim G^2$ is the photon number in the ground state [37] and $B=\frac{\lambda^2}{G^2}(\frac{\omega_b}{2\omega_a})^2\frac{2j}{2j-1}\sim 1/G^2$ and $\Delta_a=(V_1-V_0)+\frac{1}{2}(|\Delta_1|+|\Delta_0|)$ shown in Fig.1 . One can see the anomalous spectral weight $-B\sim(\lambda/G)^2$ is negative and completely due to λ (away from the Z_2 limit). So the B term in the anomalous photon correlation function can reflect precisely the anisotropy β and can be easily detected in phase sensitive Homodyne measurements [30].

Similarly, we also find the first order correction $\sim 1/G^2$ to the photon number correlation function:

$$\langle n(t)n(0)\rangle-\langle n\rangle^2=A[1+B]^2e^{-i(\omega_a+\Delta_n)t} \tag{11}$$

where $\Delta_n=(V_1-V_0)-\frac{1}{2}(|\Delta_1|-|\Delta_0|)$ shown in Fig.1 and $\langle n\rangle=A$ is the photon number in the ground state which does not receive first-order correction. From Eq.10 and 11, one can see that the Δ_0 can be directly extracted from the very first frequency in Eq.10, while $|\Delta_1|=\Delta_a-\Delta_n$ and $V_1-V_0=(\Delta_a+\Delta_n)/2-|\Delta_0|$. So all the parameters of the cavity systems such as the doublet splittings $\Delta_0(\lambda),\Delta_1(\lambda)$ and energy level shifts V_1-V_0 in Fig.1 can be extracted from the photon normal and anomalous Green functions Eq.10 and photon number correlation functions Eq.11. Their spectral weights also contain detailed information on the wavefucntions of the system's energy levels. They can be measured by photoluminescence, phase sensitive homodyne and Hanbury-Brown-Twiss (HBT) type of experiments [30] respectively.

VIII. EXPERIMENTAL REALIZATIONS AND DETECTIONS

In order to observe the parity oscillation effects, one has to move away from the Z_2 limit realized in the experiments [18–20], namely, $0<\beta<1$. This has been realized in the recent experiment [27] with $N\sim 10^5$ cold atoms inside an optical cavity which can tune β from 0 to 1. In view of recent experimental advances to manipulate a few atoms inside an optical cavity [35, 36], it should be practical to reduce the number of atoms to a few in the experiment [27]. In circuit QED systems, there are various experimental set-ups such as charge, flux, phase qubits or qutrits, the couplings could be capacitive or inductive through Λ,V,Ξ or the Δ shape [39]. Especially, continuously changing $0<\beta<1$ has been achieved in the recent experiment [25]. An shown in [8], the repulsive qubit-qubit interaction also reduces the critical coupling g_c.

From Fig.3a1, at $N=2,\beta=0.1,l=0$, one can estimate the maximum splitting between the first two zeros $\Delta_0\sim 0.1\omega_a$ which is easily experimentally measurable. Δ_l increases as $l=1,2$ as shown in Fig.3a2,a3. At $\beta=0.5$ in Fig.3b1, Δ_0 decreases to $\sim 0.01\omega_a$ which is still easily measurable. The splittings at $\beta=0.2,0.3,0.4$ falling in the range $0.01\omega_a<\Delta_0<0.1\omega_a$ are shown in the Fig.4 in the appendix C. At $\beta=0.9$ in Fig.3c1, Δ_0 decreases to $\sim 10^{-11}\omega_a$ which may become difficult to measure. However, in view of recent advances in the precision measurements in the detection of the elusive gravitational waves [38], it is also possible to measure such a tiny splitting by the phase sensitive homodyne detection [20]. So the parity oscillations can be easily experimentally measured when β is not too close to the Z_2 limit with a finite $N=2-9$ atoms or qubits inside a cavity. As said in the last section, the photon normal, anomalous and photon number correlation functions in Eq.10 and 11 can be measured by photoluminescence, phase sensitive homodyne and Hanbury-Brown-Twiss (HBT) type of experiments [30] respectively.

IX. CONCLUSIONS AND DISCUSSIONS

The four standard quantum optics models at a finite N were proposed by the old generation of great physicists many decades ago. Their importance in quantum and non-linear optics ranks the same as the bosonic or fermionic Hubbard models and Heisenberg models in strongly correlated electron systems and the Ising models in Statistical mechanics [40]. Despite their relative simple forms and many previous theoretical works, their solutions at a finite N, especially inside the superradiant regime, remain unknown. In this work, we addressed this outstanding historical problem by using the strong coupling expansion and ED. We are able to analytically calculate various photon correlation functions in the superradiant regime remarkably accurate except when β is too small where the (non)-degenerate perturbations near the $U(1)$ limit ($\beta=0$) works well [8]. The present work may inspire several new directions. From the wavefunctions listed in appendix B, it would be interesting to evaluate [32] the effects of the parity oscillations on the atom-photon entanglements at a given $l=0,1,2...$ manifold. It is important to incorporate the effects of the external pumping and cavity photon decays [30] to evaluate the photon correlations functions in Eq.10,11 using Keldysh non-equilibrium Green function approach. It would be tempting to study the arrays of cavities leading to the $Z_2/U(1)$ Dicke lattice models [41] with general $0<\beta<1$.

Acknowledgements

We acknowledge NSF-DMR-1161497, NSFC-11174210 for supports. The work at KITP was supported by NSF PHY11-25915. CLZ's work has been supported by National Keystone Basic Research Program (973 Program) under Grant No. 2007CB310408, No. 2006CB302901 and by the Funding Project for Academic Human Resources Development in Institutions of Higher Learning Under the Jurisdiction of Beijing Municipality.

In this appendix, (1) We give the derivation of Eq.4 in the main text (2) We list the wavefunctions up to the first order in $1/G^2$ in the strong coupling expansion which are needed to evaluate various photon correlation functions. (3) We also provide some additional ED results which complement to those presented in the main text.

Appendix A: Derivation of Equation 4

The first non-vanishing contribution to the off-diagonal matrix element is through $N = 2j$ order perturbation $V_{12} = V_{21} = \Delta_0(\lambda) = \langle 2|H_N|1\rangle$ where $H_N = P_0 V \frac{1-P_0}{E_0-H_0} V \cdots \frac{1-P_0}{E_0-H_0} V P_0$ which contains N interaction V and $N-1$ propagator $\frac{1-P_0}{E_0-H_0}$, E_0 is the ground state energy and P_0 is the projection onto the ground state manifold spanned by the doublets $|1\rangle$ and $|2\rangle$.

Using the eigenvalues $E^0_{l,m} = \omega_a(l-g^2_m), g_m = mG$ and inserting the eigenstates $|l\rangle_m|j,m\rangle$ of H_0 into the expression leading to

$$\Delta_0(\lambda) = -(\frac{\omega_b}{2\omega_a})^{N-1}\frac{\omega_b}{2}\sqrt{N}\sum_{\{l\}}\prod_{m=-j+1}^{j-1}[A(l_{j+m+1}, l_{j+m})]\frac{\sqrt{j(j+1)-m(m+1)}}{l_{j+m}+G^2(j^2-m^2)} \times [{}_{-j+1}\langle l_1|[|0\rangle_{-j} + \lambda|1\rangle_{-j}] \quad \text{(A1)}$$

where $A(l_{j+m+1}, l_{j+m}) ={}_{m+1}\ \langle l_{j+m+1}|1 + \lambda(a^\dagger - a)|l_{j+m}\rangle_m ={}_{m+1}\ \langle l_{j+m+1}|[|l_{j+m}\rangle_m + \lambda\sqrt{l_{j+m}+1}|l_{j+m}+1\rangle_m - \lambda\sqrt{l_{j+m}}|l_{j+m}-1\rangle_m]$, the product is over the $N-1$ intermediate states $|l\rangle_m|jm\rangle, m = -j+1, \cdots, j-1$ connecting $|1\rangle$ to $|2\rangle$ and $\{l\} = l_1, \cdot, l_{2j-1}, l_{2j} = 0$.

In the $G \gg 1$ limit, it is justified to drop the l_{j+m} dependence in the denominator, Eq.A1 is simplified to:

$$\Delta_0(\lambda) = -(\frac{\omega_b}{2\omega_a G^2})^{N-1}\frac{\omega_b}{2}\sqrt{N}\prod_{m=-j+1}^{j-1}\frac{\sqrt{j(j+1)-m(m+1)}}{j^2-m^2}\ {}_j\langle 0|[1+\lambda(a^\dagger - a)]^N|0\rangle_{-j} \quad \text{(A2)}$$

The overlapping matrix element between the two ground states can be evaluated as:

$${}_j\langle 0|[1+\lambda(a^\dagger - a)]^N|0\rangle_{-j} = \sum_{n=0}^{N}\lambda^n C^n_N E_n \quad \text{(A3)}$$

where the E_n means taking the coefficient of $x^n/n!$ in the Tylor expansion of $E(x) = e^{-(G'+x)^2/2}$ where $G' = NG$.

Taking the coefficient leads to:

$${}_j\langle 0|[1+\lambda(a^\dagger - a)]^N|0\rangle_{-j} = e^{-(G')^2/2}\sum_{l=0}^{N}\frac{N!\lambda^l}{(N-l)!}\sum_{n=0}^{[l/2]}\frac{(-1/2)^n(-\lambda G')^{l-2n}}{n!(l-2n)!} \quad \text{(A4)}$$

where $[l/2]$ is the closest integer to $l/2$.

Evaluating the product $\prod_{m=-j+1}^{j-1}\frac{\sqrt{j(j+1)-m(m+1)}}{j^2-m^2} = \frac{\sqrt{2j}}{(2j-1)!}$ in Eq.A2 leads to Eq.4.

Appendix B: The wavefunctions by strong coupling expansion.

The zero-th order ground states with even and odd parities of the system is at $l = 0, m = j$ sector in Eq.2:

$$|e\rangle_0 = \frac{1}{\sqrt{2}}[|l=0\rangle_j|j,j\rangle + |l=0\rangle_{-j}|j,-j\rangle]$$
$$|o\rangle_0 = \frac{1}{\sqrt{2}}[|l=0\rangle_j|j,j\rangle - |l=0\rangle_{-j}|j,-j\rangle] \quad \text{(B1)}$$

with the energies $E_{o/e} = E_0 + V_0(\lambda) \pm |\Delta_0(\lambda)|$ shown in Fig.1.

Using straightforward non-degenerate perturbation expansion, we find the first order correction in $1/G^2$ to the even/odd ground states at $l = 0$ in Eq.B1:

$$|\alpha\rangle_1 = \frac{\omega_b}{2\omega_a}\sqrt{2j}\sum_l\frac{{}_{j-1}\langle l|1-\lambda(a^\dagger - a)|l=0\rangle_j}{l+G^2(2j-1)}\frac{1}{\sqrt{2}}[|l\rangle_{j-1}|j,j-1\rangle + \alpha(-1)^l|l\rangle_{-j+1}|j,-j+1\rangle]$$
$$+ (\frac{\omega_b}{2\omega_a})^2 2j\sum_{l,l'\neq 0}\frac{{}_j\langle l'|1+\lambda(a^\dagger - a)|l\rangle_{j-1}\cdot{}_{j-1}\langle l|1-\lambda(a^\dagger - a)|l=0\rangle_j}{l'[l+G^2(2j-1)]}\frac{1}{\sqrt{2}}[|l'\rangle_j|j,j\rangle + \alpha(-1)^{l'}|l'\rangle_{-j}|j,-j\rangle] \quad \text{(B2)}$$

where $\alpha = \pm$ for $\alpha = e/o$ respectively. Indeed, it shows that the even (odd) parity ground state is mixed with only other even (odd) parity states as dictated by the parity conservation of the Hamiltonian at any finite N. One can see the first-order correction to the ground state wavefunction consists of two parts: the first part (line) is in the high energy optical sector, the second part (line) is in the low energy atomic sector.

The zero-th order l-th level states with even and odd parities of the system is at $l, m = j$ in Eq.2:

$$
\begin{aligned}
|e, l\rangle &= \frac{1}{\sqrt{2}}[|l\rangle_j |j, j\rangle + (-1)^l |l\rangle_{-j} |j, -j\rangle] \\
|o, l\rangle &= \frac{1}{\sqrt{2}}[|l\rangle_j |j, j\rangle - (-1)^l |l\rangle_{-j} |j, -j\rangle]
\end{aligned}
\tag{B3}
$$

with the energies $E_{o/e} = E_l^0 + V_l(\lambda) \pm |\Delta_l(\lambda)|, E_l^0 = \omega_a[l - (Gj)^2]$ in Fig.1.

Similarly, one can find the first order correction to the two doublets at $l = 1$ in Eq.B3 by making the following replacements in Eq.B2: (1) changing $|l = 0\rangle_j$ to $|l = 1\rangle_j$ (2) the denominator $[l + G^2(2j - 1)]$ to $[l - 1 + G^2(2j - 1)]$. (3) the sum subscript $l' \neq 0$ to $l' \neq 1$.

These wavefunctions are used to calculate the photon correlation functions Eq.10 and 11.

Appendix C: Some additional Exact Diagonization results

In this appendix, we show the results on even/odd splitting Δ_l for $N = 2$ at $\beta = 0.2, 0.3, 0.4$ at $l = 0, 1, 2$. They make up the results between $\beta = 0.1$ and $\beta = 0.5$ shown in Fig.3 in the main text. Especially, they describe how the maximum splitting between the first two zeros Δ_0 monotonically decreases from $\Delta_0 \sim 0.1\omega_a$ at $\beta = 0.1$ to $\Delta_0 \sim 0.01\omega_a$ at $\beta = 0.5$, also how the other zeros separate from the first two as β increases.

We also made the comparisons between strong coupling expansions and the ED on the doublet splittings for $N = 5$ at $\beta = 0.1, 0.5, 0.9, 1$ and $l = 0, 1, 2$ and found similar agreements as those at $N = 2$ shown in Fig.3.

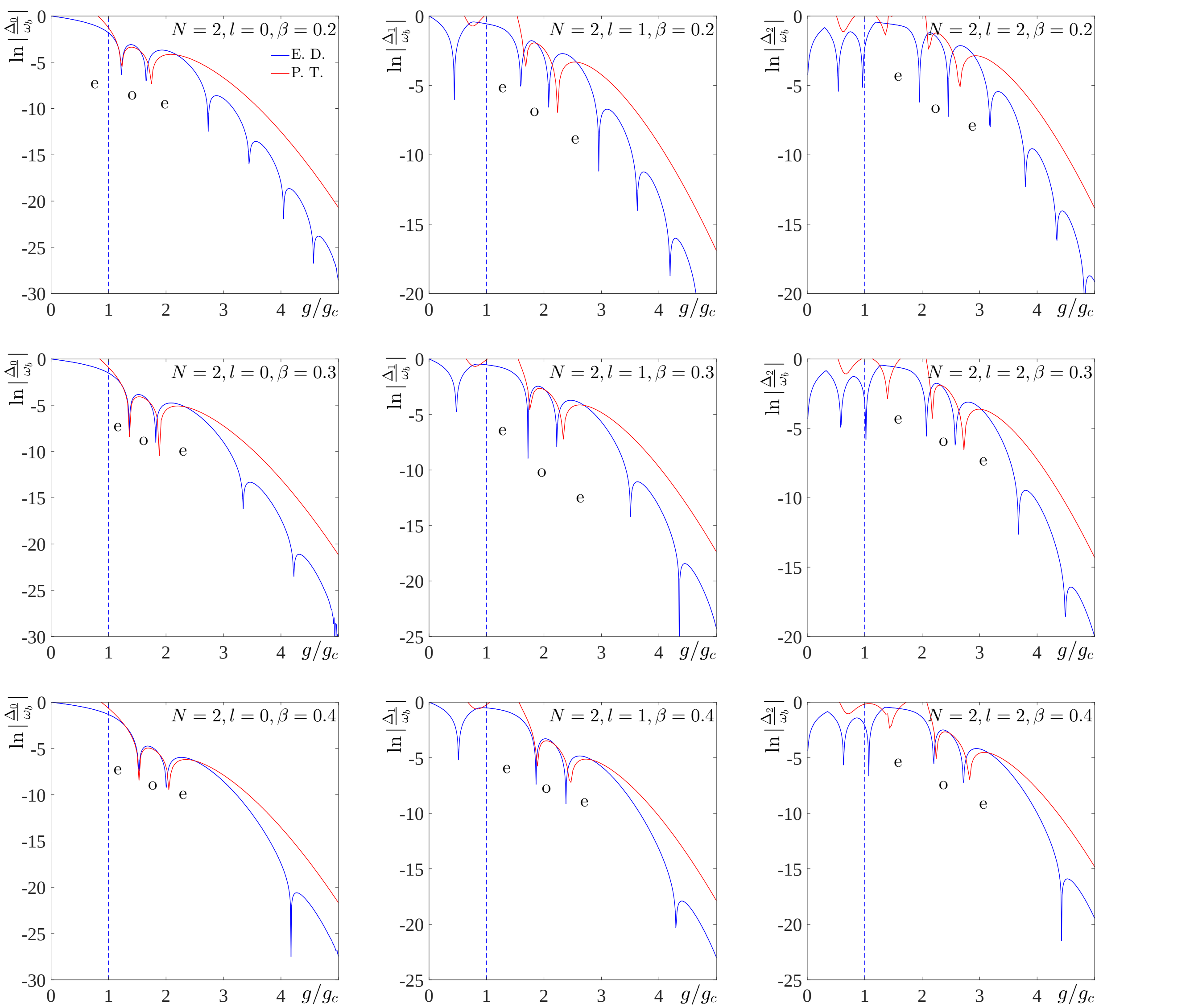

FIG. 4. (Color Online) The even/odd splitting Δ_l for $N=2$ at $\beta=0.2, 0.3, 0.4$ at $l=0,1,2$ in the Log scale $\ln|\frac{\Delta_l}{\omega_b}|$ versus g/g_c. The notations are the same as those in Fig.3. The strong coupling expansion works very well in the ground state doublet $l=0$. There are some small deviations form the ED at the excited doublets $l=1,2$ when $\beta=0.2$, but the deviations decrease when $\beta=0.3, 0.4$. As β increases, the other zeros start to gradually move away from the first two. As shown in the main text, all the splittings are easily experimentally measurable.

[1] D. F. Walls and G. J. Milburn, Quantum Optics, Springer-Verlag, 1994.
[2] M. O. Scully and M. S. Zubairy, Quantum Optics, Cambridge University press, 1997
[3] I.I. Rabi, Phys. Rev. 49, 324 (1936); 51, 652 (1937).
[4] E. T. Jaynes and F. W. Cummings, Proc. IEEE 51, 89 (1963).
[5] R.H. Dicke, Phys. Rev. 93, 99 (1954)
[6] M. Tavis and F.W. Cummings, Phys. Rev. 170, 379 (1968).
[7] Jinwu Ye and CunLin Zhang, Phys. Rev. A 84, 023840 (2011).
[8] Yu Yi-Xiang, Jinwu Ye and W.M. Liu, Scientific Reports 3, 3476 (2013).
[9] Yu Yi-Xiang, Jinwu Ye, W.M. Liu and CunLin Zhang, arXiv:1506.06382.
[10] K. Hepp and E. H. Lieb, Anns. Phys. (N. Y.), 76, 360 (1973); Y. K. Wang and F. T. Hioe, Phys. Rev. A, 7, 831 (1973).
[11] V. N. Popov and S. A. Fedotov, Soviet Physics JETP, 67, 535 (1988); V. N. Popov and V. S. Yarunin, Collective Effects in Quantum Statistics of Radiation and Matter (Kluwer Academic, Dordrecht,1988).
[12] C. Emary and T. Brandes, Phys. Rev. Lett. 90, 044101 (2003); Phys. Rev. E 67, 066203 (2003). N. Lambert, C. Emary, and T. Brandes, Phys. Rev. Lett. 92, 073602 (2004).
[13] J. Vidal and S. Dusuel, Europhys. Lett. 74, 817 (2006). For the Z_2 Dicke model $\beta = 1$, the ground state photon number at the QCP was found to scale as $\langle n_{ph} \rangle \sim cN^{1/3}$[13] which is a direct consequence of finite size scaling near a QCP with infinite coordination numbers [14]. For the general $U(1)/Z_2$ Dicke model Eq.1 with $0 < \beta < 1$, the normal to the superradiant transitions at $N = \infty$ share the same universality class as the Z_2 limit at $\beta = 1$, so only the coefficient c depends on β. As shown in this paper, the dramatic qualitative differences and new phenomena due to $\beta \neq 1$ show up only away from the QCP in the super-radiant regime.
[14] R. Botet, R. Jullien, and P. Pfeuty, Phys. Rev. Lett. 49, 478 (1982); Phys. Rev. B, 28, 3955 (1983).
[15] There is a "formal" exact solution on the Z_2 Dicke model at $N = 1, \beta = 1$. D. Braak, Phys. Rev. Lett. 107, 100401 (2011). Unfortunately, this exact solution is essentially useless in any practical computations. It is also difficult to extract any physics from it. For example, it is difficult to even derive $\langle n_{ph} \rangle \sim N^{1/3}$ scaling near the QCP [13] and also any new phenomenon achieved in the present paper in the super-radiant regime from the formally exact solution even at the simplest case $N = 1, \beta = 1$. It would be impossible to calculate the dynamic photon correlation functions Eq.10,11.
[16] F. Brennecke, *et.al*, Nature 450, 268 - 271 (08 Nov 2007);
[17] Yves Colombe, *et.al*, Nature 450, 272 - 276 (08 Nov 2007).
[18] A. T. Black, H. W. Chan and V. Vuletic, Phys. Rev. Lett. 91, 203001(2003).
[19] K. Baumann, *et.al*, Nature 464, 1301-1306 (2010);
[20] K. Baumann, *et.al*, Phys. Rev. Lett. 107, 140402 (2011).
[21] A. Wallraff, *et.al*, Nature 431, 162-167 (2004)
[22] G. Gunter, *et.al*, Nature, Vol 458, 178, 12 March 2009.
[23] Aji A. Anappara, *et.al*, Phys. Rev. B 79, 201303(R) (2009).
[24] Reithmaiser, J. P, *et.al*, Nature 432, 197-200 (2004); Yoshie, T. *et al*, Nature 432, 200-203 (2004); K. Hennessy, *et al*, Nature 445, 896-899 (22 February 2007).
[25] T. Niemczyk, *et.al*, Nature Physics 6,772-776(2010).
[26] F. Dimer, *et.al*, Phys. Rev. A, 75, 013804, 2007
[27] Markus P. Baden, *et.al*, Phys. Rev. Lett. 113, 020408 (2014).
[28] For strong coupling expansions and spin wave expansion in spin-orbit coupled lattice systems, see Fadi Sun, Jinwu Ye, Wu-Ming Liu, Phys. Rev. A 92, 043609 (2015); arXiv:1502.05338.
[29] Qing-Hu Chen, Yu-Yu Zhang, Tao Liu and Ke-Lin Wang, Phys. Rev. A 78, 051801(R) (2008).
[30] Jinwu Ye, T. Shi and Longhua Jiang, Phys. Rev. Lett. 103, 177401 (2009); T. Shi, Longhua Jiang and Jinwu Ye, Phys. Rev. B 81, 235402 (2010); Jinwu Ye, Fadi Sun, Yi-Xiang Yu and Wuming Liu, Ann. Phys. 329, 51C72 (2013).
[31] It is tempting to try to sort out if there is an extra symmetry at the Z_2 limit $\beta = 1$. Taking the Eq.1, one can see the last two terms exchange under the transformation $a \to e^{i\pi/2}a, \sigma_- \to e^{i\pi/2}\sigma_-$. It is also easy to see the Hamiltonian has the symmetry $\mathcal{T} \times R(y, \pi)$ or $\mathcal{T} \times R(x, \pi) \times Z_2^a$ where $\mathcal{T}$ is the Time reversal symmetry, $R(y, \pi), R(x, \pi)$ are the spin rotations by π around y or x axis respectively and Z_2^a is $a \to -a$. So there is no extra symmetry at the Z_2 limit.
[32] Yu Yi-Xiang, Jinwu Ye and CunLin Zhang, unpublished.
[33] C. Monroe, *et.al*, Science 24 May 1996: 1131-1136; D. Leibfried, E. Knill, S. Seidelin, J. Britton, *et.al*, Nature 438, 639-642 (1 December 2005).
[34] J. R. Friedman, *et.al*,, Nature 406, 43-46 (6 July 2000). Caspar H. van der Wal, *et.al*, Science 27 October 2000: 773-777.
[35] W. S. Bakr, *et.al*, Science 30 July 2010: 547-550.
[36] F. Serwane, *et.al*, Science 15 April 2011: 336-338.
[37] In the first line in Eq.10, setting $t = 0$ and using $[a, a^\dagger] = 1$, one can also see the photon number in the ground state $\langle n \rangle = A$.
[38] B. P. Abbott et al. (LIGO Scientific Collaboration and Virgo Collaboration), Phys. Rev. Lett. 116, 061102 (2016).
[39] For reviews, see J. Q. You, Franco Nori, Nature 474, 589 (2011). Steven M. Girvin, Superconducting Qubits and Circuits: Artificial Atoms Coupled to Microwave Photons, Lectures delivered at Ecole dEte Les Houches, July 2011. To be published by Oxford University Press.
[40] A. Auerbach, *Interacting electrons and quantum magnetism*, (Springer Science & Business Media, 1994).
[41] M. Schir, M. Bordyuh, Bztop, H. E. Tureci, Phys. Rev. Lett. 109, 053601 (2012), For a review on experimnetal implementations, see, Andrew A. Houck, Hakan E. Tureci and Jens Koch, Nature Physics 8, 292299 (2012).